A Lead-Free and High-Energy Density Ceramic for Energy Storage Applications

Correia, T. M., McMillen, M., Rokosz, M. K., Weaver, P. M., Gregg, M., Viola, G., & Cain, M. G. (2013). A Lead-Free and High-Energy Density Ceramic for Energy Storage Applications. Journal of the american ceramic society, 96(9), 2699-2702. https://doi.org/10.1111/jace.12508

Published in:
Journal of the american ceramic society

Document Version:
Early version, also known as pre-print

Queen's University Belfast - Research Portal:
Link to publication record in Queen's University Belfast Research Portal

A lead-free and high energy density ceramic for energy storage applications

T. M. Correia[1]*, M. McMillen[2], M. K. Rokosz[1], P.M. Weaver[1], M. Gregg[2], G. Viola[3,4], Markys G Cain[2]

[1]National Physical Laboratory, Hampton Road, Teddington, Middlesex TW11 0LW, UK

[2]Centre for Nanostructured Media, School of Maths and Physics, Queen's University Belfast, Belfast,

BT7 1NN, Northern Ireland, United Kingdom

[3] School of Engineering and Materials Science, Queen Mary University of London, Mile End Road,

London E1 4NS, UK

[4] Nanoforce Technology Ltd, Queen Mary University of London, Mile End Road, London E1 4NS, UK

*corresponding author: tatiana.correia@npl.co.uk

Abstract

In this work we demonstrate a very high energy density and high temperature stability capacitor based on $SrTiO_3$ substituted $BiFeO_3$ thin films. An energy density of 18.6 J/cm^3 at 972 kV/cm is reported. The temperature coefficient of capacitance (TCC) was below 11% from room temperature up to 200 °C. These results are of practical importance, because it puts forward a promising novel and environmentally friendly, lead-free material, for high temperature applications in power electronics up to 200 °C. Applications include capacitors for low carbon vehicles, renewable energy technologies, integrated circuits, and for the high temperature aerospace sector.

Introduction

Energy storage systems play an important role in the sustainable energy program as these can enable more efficient use of energy generated from renewable sources, which in turn, supports the

stabilization of the energy market and reduces its environmental impact. Capacitors are a promising technology for energy storage devices as they are characterized by high power density and fast charge/discharge time (>1 μs) compared to batteries [1-3]. They are also low cost, and more thermally and mechanically robust. Although dielectrics can store significantly less *energy* than Li batteries, fuel cells and supercapacitors, they have been proposed for use in high-power applications such as defibrillators, detonators, power electronics, etc [1-4]. In recent years there has been a drive to develop new capacitor materials with very high dielectric constant and energy storage capacity to support these new applications [3, 5-10].

The energy density *U* of a dielectric is defined as:

$$\square = \int \square\square\square \tag{1}$$

where $\square = \square_0\square + \square$. For ferroelectric base compounds where *P* is high, $\square \approx \square$. Thus,

$$\square = \int \square\square\square \tag{2}$$

where *E* is the applied electric field that causes a variation of electric displacement *dD* or polarization *dP*. From equation 2 we note that the highest energy density *U* in any dielectric is dependent on a high dielectric breakdown field and both a high maximum (with a low remanent) polarization. Electrolytic capacitors are widely used because, although the oxide film dielectric has a low permittivity, it can sustain a large electric field. This, combined with a large surface area, results in a high specific capacitance and energy density relative to ceramic-based dielectrics. Nevertheless, these capacitors have some serious limitations. The maximum operating temperature is typically 85 °C, but the lifetime and reliability are seriously impaired at these temperatures. This constraint has been tackled by attempting to replace electrolytics by ceramic-based dielectrics, as these are more temperature and vibration robust than the former. Due to the fact that ceramics are characterized by a low energy density, much effort has been devoted, in the last decade, to the development of high energy density ceramic materials [3, 5-10]. Antiferroelectric and relaxor doped-PZT (Lead-

zirconate titanate) ceramics stand out for their impressive energy density (up to 58.1 J/cm^3 at 2805 kV/cm) [10], but political and environmental demands are pushing the development towards lead-free materials. In this paper, we report on the development of a new lead-free, high energy density dielectric material. Our approach capitalizes on the characteristic high polarization of the $BiFeO_3$ lattice and the decrease of its remanent polarization through Bi and Fe substitution. In this work we present the investigations carried out on the energy density in $0.4BiFeO_3$-$0.6SrTiO_3$ (abbreviated as BFST) thin film.

Experimental Method

A ceramic target with composition $(BiFeO_3)_{0.4}$-$(SrTiO_3)_{0.6}$ was processed by solid state reaction with Bi_2O_2, Fe_2O_3 and $SrTiO_3$ as starting powders. The powders were milled and calcined at 700 °C. The calcined powder was uniaxially pressed and further sintered at 1100 °C for 30 min in air furnace. BFST thin film was prepared onto a $SrRuO_3$ (50 nm) electroded (100)-$SrTiO_3$ substrate by Pulsed Laser Deposition (PLD) method and using a KrF excimer laser (λ=248 nm) operated with pulse repetition rate of 10 Hz. After being deposited at 650 °C and under 0.027 mbar O_2 pressure, the film was post-annealed at 450 °C for 30 minutes under 800 mbar O_2. The stoichiometry $(BiFeO_3)_{0.4}$-$(SrTiO_3)_{0.6}$ was targeted, however EDX results (see in Ref. 11) suggested that the resulting thin film was bismuth deficient and strontium rich than the nominal composition. Circular top electrodes of Platinum (500 µm diameter) were evaporated through a patterned mask. The layer structure of the film is $SrTiO_3$/$SrRuO_3$/BFST/Pt. Permittivity and dielectric losses measurements were performed using an impedance analyzer (Agilent 4294 A, Precision Impedance Analyzer), attached to a probe station (Suss MicroTec - ProbeShield PM8). A hotplate was used for temperature control (att Systems – A200). *P-E* loops were acquired by means of a Radiant Technologies RT66A ferroelectric tester at 1 kHz.

Results and discussion

High Temperature Stability

Figure 1 shows the temperature dependence of the relative permittivity and dielectric loss measured in a BFST thin film (of thickness 400 nm measured by cross-sectional TEM-EDX) for various frequencies. The inset of Figure 1 shows a large frequency dispersion of permittivity and dielectric losses (tan δ), within a small frequency window. The loss, tan δ linearly increases with the frequency and is < 5% in excess of 12 kHz. The significant increasing of tan δ for frequencies above 12 kHz suggests the contribution from extrinsic impedance, like electrodes. The relative permittivity ranged from 880 (30 kHz) to a maximum of 980 (10 kHz) at T_m=90 °C and showed frequency dispersion, which suggest that a diffuse relaxation mechanism takes place. Fedulov et al. [12] extensively studied the $(BiFeO_3)_{1-x}$-$(SrTiO_3)_x$ ceramic phase diagram by X-Ray Diffraction and dielectric measurements. The author found that $(BiFe0_3)_{0.4}$-$(SrTiO_3)_{0.6}$ ceramics exhibit two permittivity maxima at T_{m1}=200°C and T_{m2}=400 °C, the temperature at which broad permittivity peaks were observed. In our thin film, and within the measured temperature range, we observed a single permittivity maximum at a lower temperature ~ 90 °C characterized by frequency dispersion. The discrepancy between our results and the ones reported by Fedulov [12] may be due to the bismuth deficient composition of our film, placing it in a different position in the phase diagram. Fedulov's results showed that, for Strontium-rich compositions, T_{m1} can extend below 100 °C. Fedulov's phase diagram is a single degree of freedom system where the Bi:Fe and Sr:Ti ratios are fixed at 1:1. Bi loss would result in a deviation from these fixed ratios, placing us in a different part of the full three degrees of freedom phase diagram. Also, we cannot neglect the contribution of film strain induced by the substrate to the transition temperature, which is recognized to play an important role in the paraelectric-ferroelectric structural phase transitions and relaxation mechanisms [13].

An important observation given by Figure 1, is that the permittivity of the BFST thin film remains within the 9-11 % of its room temperature value up to 200 °C. With a temperature coefficient of

capacitance, *TCC*, of 9-11%, BFST thin films potentially places itself in an advantageous position compared to currently available commercial devices. The X*N*R capacitors (*N*=6, 7, 8,) temperature rating of capacitors specifies a maximum deviation of 15% from room temperature value at the rated temperature. X7R rated capacitors are widely available and maintain their capacitance to within 15% of room temperature value up to 125 °C. X8R capacitors maintain their capacitance to within 15% up to 150 °C and are available as a speciality product [www.syfer.com]. X9R capacitors (15% up to 200 °C) are not commercially available. Ceramic capacitors with operating temperatures up to 200 °C are available but suffer a large diminution (65%) of capacitance at the upper temperature limit. This presents a serious limitation on the use of ceramic capacitors for high temperature applications such as operating high temperature power conversion electronics. We believe that our BFST thin film is a promising capacitor candidate for high temperature applications, as demanded by industries including low carbon vehicles, renewable energies, integrated circuits, and high temperature environments associated with aerospace applications, for example.

Energy Density and Efficiency

Figure 2 shows a slim and partially-saturated *P-E* loop obtained in BFST thin film at room temperature. As shown, the BFST thin film is characterized by high maximum polarization P_{max} (52 μC/cm^2) and low remanent polarization P_r (3 μC/cm^2), while an electric field of 972 kV/cm is applied. From a technological perspective, the energy storage performance of a capacitor is based on the amount of energy (and power) it can release within the application constraints (e.g. rated voltage, operating temperature). Ferroelectric materials typically display hysteretic *P-E* loops where the charging (*E* increasing) and discharging (*E* decreasing) paths are not coincident (see **Figure 2**). The area of the loop represents an energy loss so that the energy delivered to the capacitor is larger than the energy that can be recovered. Therefore, recoverable energy density, during discharging, and efficiency □ (□ = $\frac{□_{□□□□□□□□□□}}{□_{□□□□□□□□□}} \times 100$), are important metrics to benchmark dielectrics for use in

energy storage devices. **Figure 3** presents the recoverable energy density *U* calculated from the integration of the quadrant of the *P*-*E* loop associated with the discharge process (*E*>0 and decreasing from its maximum). At *E*= 972 kV/cm, BFST thin films can release as much as 18.6 J/cm^3 (~ 0.72 Wh/kg) with an efficiency above 85%.

It is expected that a much higher energy density can be achieved in the BFST thin films at higher electric fields. We believe that this can be achieved by improving the quality of the film and its electrical contacts, which would act to enhance the material's dielectric breakdown strength. Such an enhancement has been observed in PLZST thick films, whose energy density was enhanced when the film was deposited on $LaNiO_3$/Si(100) and Nickel foils [10, 14]. Additionally, the utilisation of 'dead layers', manifest at ferroelectric thin film/electrode interfaces, to increase energy density has recently been reported in BFST thin films with an associated increase of up to 30% energy density [11].

Combined with the characteristic recoverable energy density and efficiency, other parameters play an important role in the performance of a capacitor, such as the voltage rating, operating temperature, cost and environmental impact. To benchmark the capability of BFST thin films for use in energy storage devices, we plot in **Figure 4** the energy density measured in BFST thin film with a number of promising films previously reported. The energy density in the BFST thin films reported here is significantly better than previously reported lead-free materials at comparable electric field [6,9]. The energy density is similar that of lead-bearing PZN-PMN-PT [2] and PLZT [3] at comparable electric fields, but this is achieved in a lead-free material. Significantly higher energy densities have been reported for PLZT at very high electric field close to electrical breakdown [10,14], but again these materials are lead-based which may have severe environmental implications. If similar methods to enhance electrical breakdown field were applied to the BFST reported here, comparable energy density would be expected using a lead-free material. The BFST material reported here presents an environmentally friendly (lead-free), inexpensive (compared to scandium based

materials for example, which is an expensive element) and thermally and mechanically stable (compared with polymers) solution for ceramic capacitors.

Conclusions

A new $(BiFeO_3)_{0.4}$-$(SrTiO_3)_{0.6}$ thin film has been developed using PLD processing routes. Its performance as a dielectric material for energy storage in capacitor applications has been investigated. High permittivity and loss (tan δ) values (up to 1000 and 0.2 respectively) were measured, and a relaxation mechanism at T_m~ 90 °C was observed as a broad peak in the permittivity/T response. These BFST thin films are also characterized by a low TCC (11%) up to 200 °C. High recoverable energy density (18.6 J/cm^3) and efficiency (85%) in BFST thin films were calculated from *P-E* data upon the application of an electric field of 972 kV/cm. We propose BFST thin films as a promising candidate for use in capacitors in power systems for high temperature applications.

Acknowledgements

This work was funded through the UK's National Measurement Office and the Technology Strategy Board under the project 'Advanced Ceramics for Energy Storage'.

References

[1] S. Kwon, W. Hackenberger, E. Alberta, E. Furman, M. Lanagan, Nonlinear Dielectric Ceramics and Their Applications to Capacitors and Tunable Dielectrics, IEEE Electrical Insulation Magazine, 27, 43 (2011)

[2] K. Yao, S. Chen, M. Rahimabady, M. S. Mirshekarloo, S. Yu, F. E. H. Tay, T. Sritharan, L. Lu, Nonlinear Dielectric Thin Films for High-Power Electric Storage With Energy Density Comparable

With Electrochemical Supercapacitors, IEEE Transactions on Ultrasonics, Ferroelectrics, and Frequency Control, 58, 1968 (2011)

[3] B. Chu, X. Zhou, K. Ren, B. Neese, M. Lin, Q. Wang, F. Bauer, Q. M. Zhang, A Dielectric Polymer with High Electric Energy Density and Fast Discharge Speed, Science, 313, 334 (2006)

[4] Joseph P. Dougherty, Cardiac defibrillator with high energy storage antiferroelectric capacitor, US Patent 5 545 184, Aug. 13, 1996

[5] M. S. Mirshekarloo, K. Yao, T. Sritharan, Large strain and high energy storage density in orthorhombic perovskite $(Pb_{0.97}La_{0.02})(Zr_{1-x-y}Sn_xTi_y)O_3$ antiferroelectric thin films, Appl. Phys. Lett. 97, 142902 (2010)

[6] N. Ortega, A. Kumar, J. F. Scott, D. B. Chrisey, M. Tomazawa, S. Kumari, D. G. B. Diestra, R. S.Katiyar, Relaxor-ferroelectric superlattices: high energy density capacitors, J. Phys.: Condens. Matter 24, 445901 (2012)

[7] J. Parui, S. B. Krupanidhi, Enhancement of charge and energy storage in sol-gel derived pure and La-modified $PbZrO_3$ thin films, Appl. Phys. Lett. 92, 192901 (2008)

[8] G. Viola, H. Ning, M J Reece, R Wilson, T M Correia, P Weaver, M G Cain, H Yan, Reversibility in electric field-induced transitions and energy storage properties of bismuth-based perovskite ceramics, J. Phys. D: Appl. Phys. 45, 355302 (2012)

[9] H. Ogihara, C. A. Randall, S. Trolier-McKinstry, High-Energy Density Capacitors Utilizing 0.7 $BaTiO_3$–0.3 $BiScO_3$ Ceramics, J. Am. Ceram. Soc. 92, 1719–1724 (2009)

[10] Y. Wang, X. Hao, J. Yang, J Xu, D. Zhao, Fabrication and energy-storage performance of $(Pb,La)(Zr,Ti)O_3$ antiferroelectric thick films derived from polyvinylpyrrolidone-modified chemical solution, J. Appl. Phys. 112, 034105 (2012)

[11] M. McMillen, A. M. Douglas, T. M. Correia, P. M. Weaver, M. G. Cain, J. M. Gregg, Increasing recoverable energy storage in electroceramic capacitors using “dead-layer” engineering, Appl. Phys. Lett. 101, 242909 (2012)

[12] S. A. Fedulov, L. I. Pyatigorskaya, Y. N. Venevtsev, An investigation of the $BiFeO_3$-$SrTiO_3$ system, Sov. Phys – Crystallography 10, 238 (1965)

[13] J. H. Haeni, P. Irvin, W. Chang, R. Uecker, P. Reiche, Y. L. Li, S. Choudhury, W. Tian, M. E. Hawley, B. Craigo, A. K. Tagantsev, X. Q. Pan, S. K. Streiffer, L. Q. Chen, S. W. Kirchoefer, J. Levy, & D. G. Schlom, Room-temperature ferroelectricity in strained $SrTiO_3$, Nature 430, 758 (2004)

[14] B. Ma, D. K. Kwon, M. Narayanan, U. B. Balachandran, Dielectric properties and energy storage capability of antiferroelectric $Pb_{0.92}La_{0.08}Zr_{0.95}Ti_{0.05}O_3$ film-on-foil capacitors, J. Mater. Res. 24, 2993 (2009)

[15] J. Sigman, G. L. Brennecka, P. G. Clem, B. A. Tuttle, Fabrication of Perovskite-Based High-Value Integrated Capacitors by Chemical Solution Deposition, J. Am. Ceram. Soc., 91, 1851 (2008)

Figure Captions

Figure 1 Temperature dependence of relative permittivity and tan δ measured at frequencies 10-30 kHz (increasing frequency is indicated by the arrow marked *f*) and at V_{ac}=0.5 V. **Inset:** Relative permittivity and tan δ as a function of frequency at room temperature.

Figure 2 *P-E* loop measured in BFST thin film at room temperature and at 1 kHz. P_{max}- maximum polarization; P_r- remanent polarization.

Figure 3 Recoverable energy density *U* as a function of *E*. Calculated from depolarizing *P-E* data (*E*>0) in Figure 1.

Figure 4 Energy density *U* as a function of *E* measured for BFST thin film and other ferroelectric and antiferroelectric thin and thick films (Refs. 2, 3, 6, 7, 9 , 10). * near breakdown field.

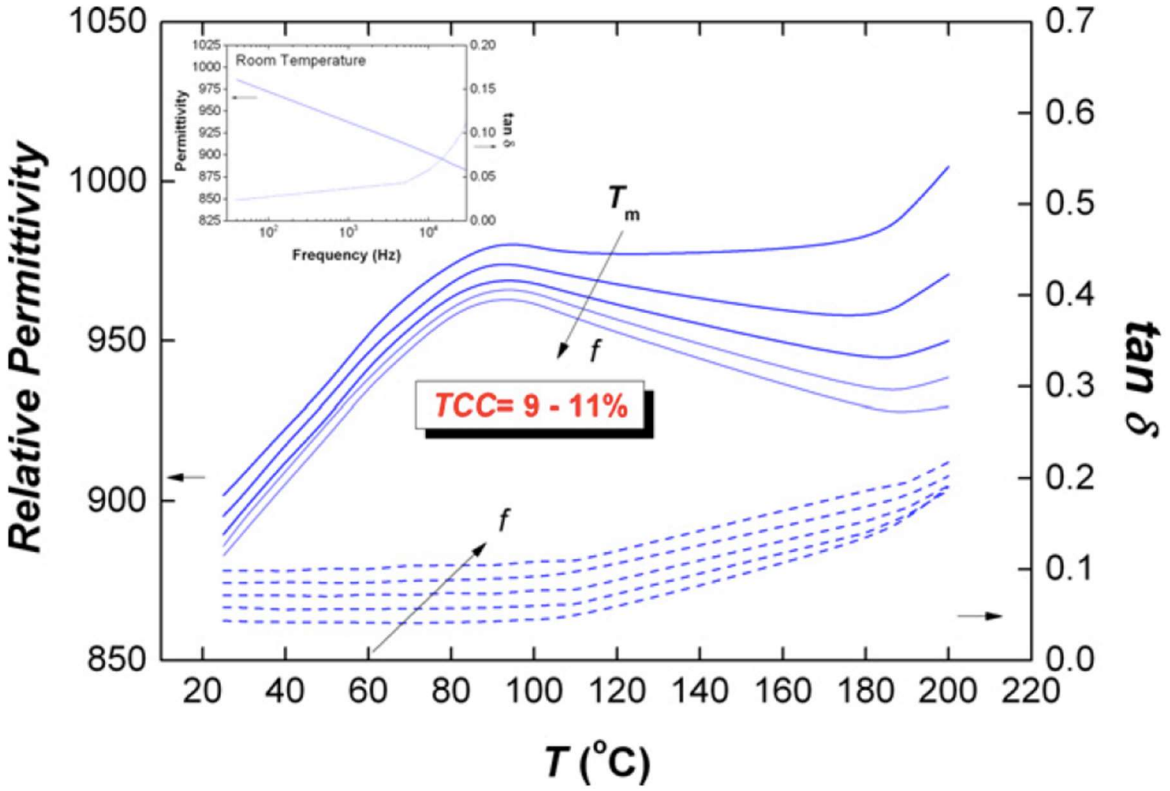
Relative Permittivity
tan δ
T (°C)
Room Temperature
Permittivity
tan δ
Frequency (Hz)
T_m
f
f
TCC= 9 - 11%

Figure 1 of 4

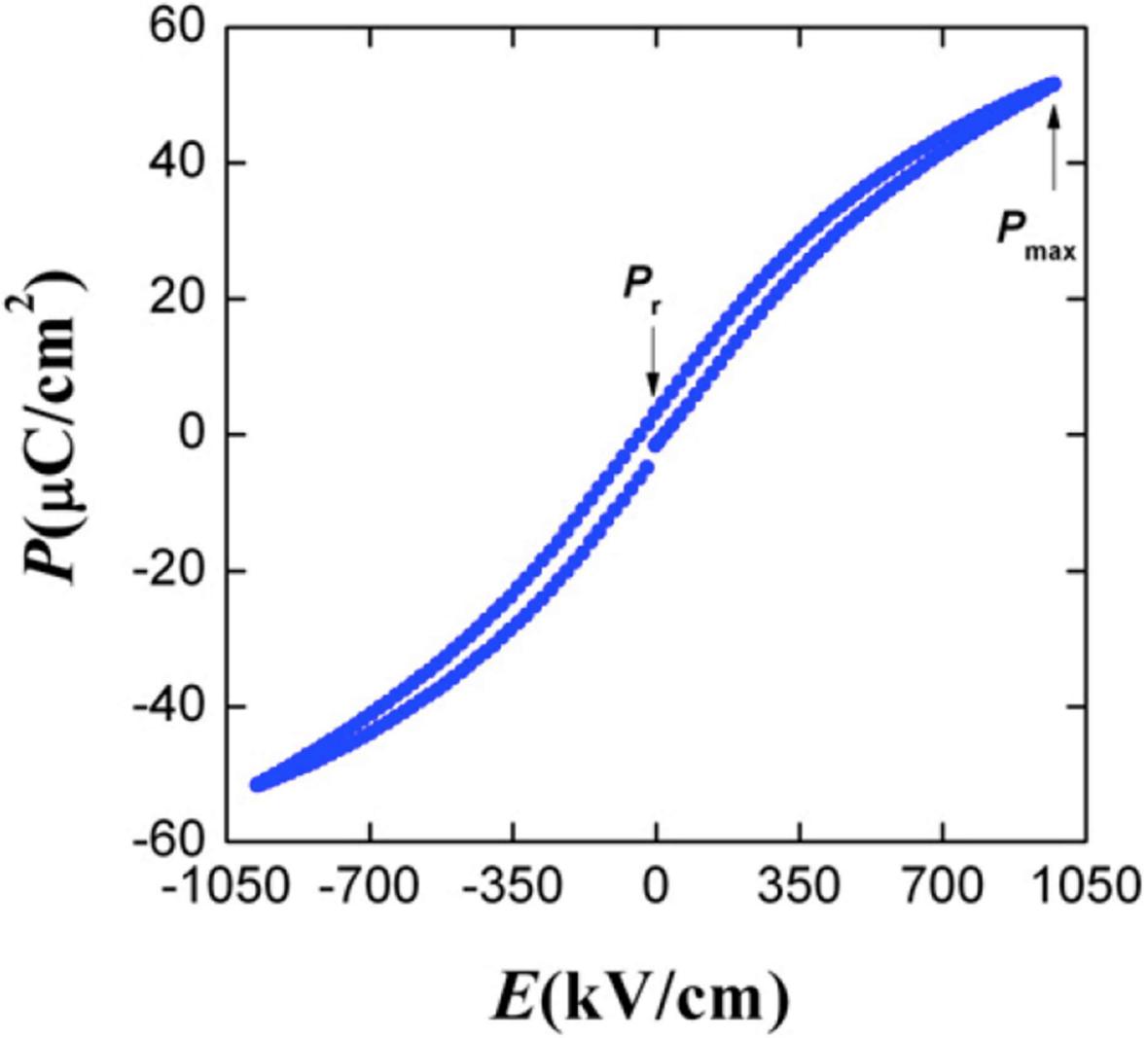
60
40
20
0
-20
-40
-60
-1050
-700
-350
0
350
700
1050
P(μC/cm²)
E(kV/cm)
P_r
P_max

Figure 2 of 4

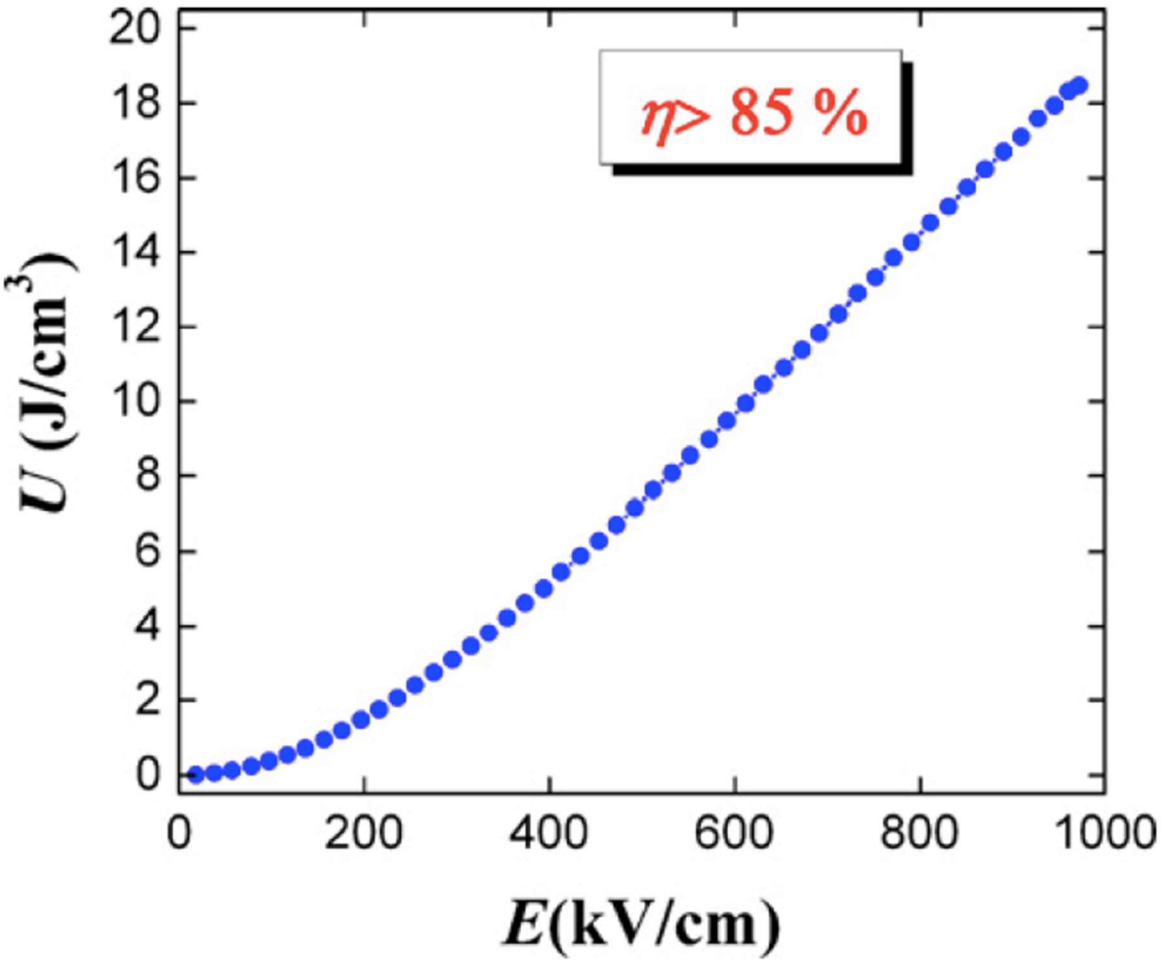

Figure 3 of 4

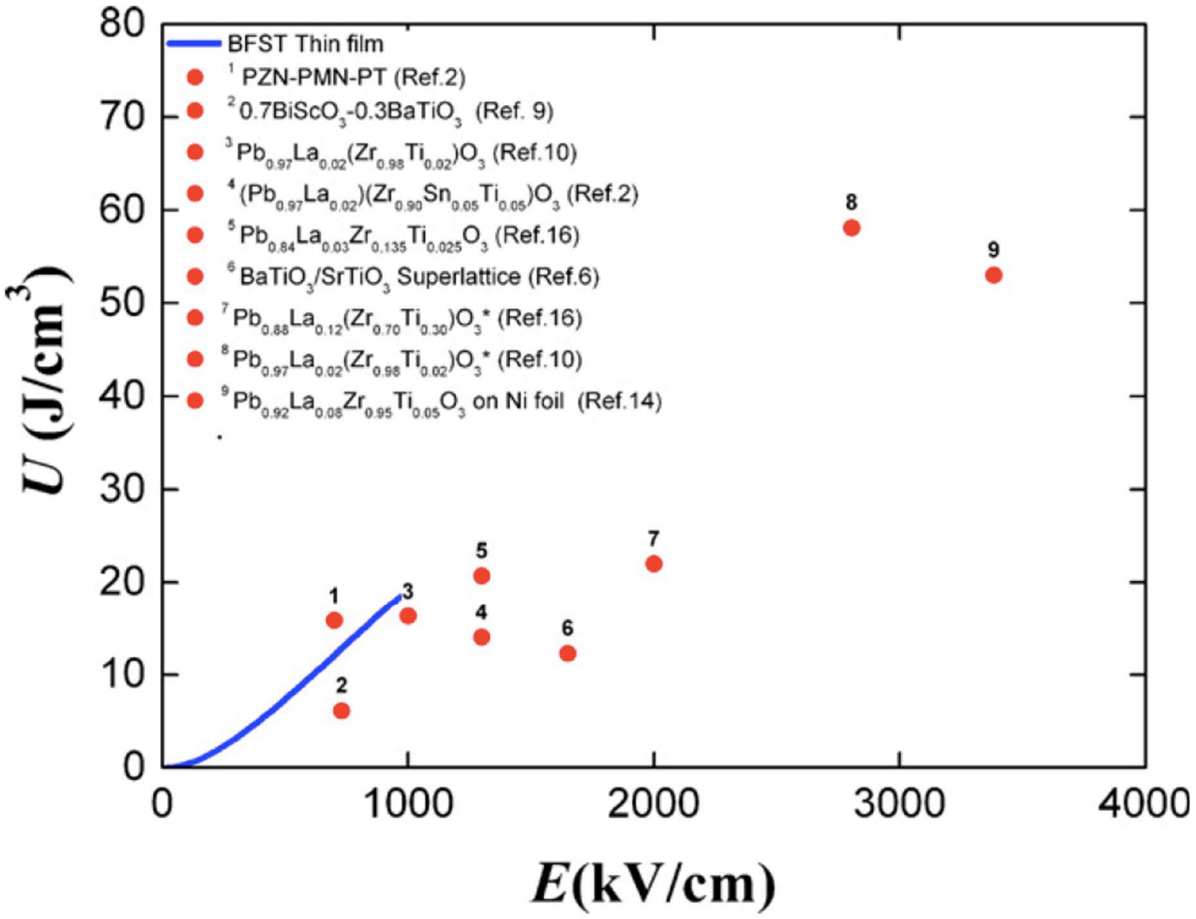
BFST Thin film
1 PZN-PMN-PT (Ref.2)
2 0.7BiScO3-0.3BaTiO3 (Ref. 9)
3 Pb0.97La0.02(Zr0.98Ti0.02)O3 (Ref.10)
4 (Pb0.97La0.02)(Zr0.90Sn0.05Ti0.05)O3 (Ref.2)
5 Pb0.84La0.03Zr0.135Ti0.025O3 (Ref.16)
6 BaTiO3/SrTiO3 Superlattice (Ref.6)
7 Pb0.88La0.12(Zr0.70Ti0.30)O3* (Ref.16)
8 Pb0.97La0.02(Zr0.98Ti0.02)O3* (Ref.10)
9 Pb0.92La0.08Zr0.95Ti0.05O3 on Ni foil (Ref.14)
U (J/cm3)
E(kV/cm)
0
10
20
30
40
50
60
70
80
0
1000
2000
3000
4000

Figure 4 of 4